

# Thin Sol-Gel Silica Films on (3-Mercaptopropyl)trimethoxysilane-Modified Ag and Au Surfaces

Wade R. Thompson and Jeanne E. Pemberton\*

Department of Chemistry, University of Arizona, Tucson, Arizona 85721

Received July 6, 1994<sup>Ⓢ</sup>

The results presented here demonstrate the utility of (3-mercaptopropyl)trimethoxysilane (3MPT) for attachment of a strongly adherent thin layer of silica to Ag and Au surfaces. The thin silica surfaces are formed by standard sol-gel procedures and are shown to be representative of other silica systems. The basis of the adhesion between these two surfaces is covalent bonding between the 3MPT and both the metal and the silica. If 3MPT is not used, the thin silica layer is poorly adherent to the Au surface and only moderately adherent to the Ag surface. Ellipsometry, X-ray photoelectron spectroscopy, Raman spectroscopy, scanning electron microscopy, and qualitative and quantitative adhesion tests are used to characterize this system.

## Introduction

Creating a strong durable bond between metal and dielectric (i.e., ceramic and glass) materials has been of continued interest for a range of applications such as electronics packaging and integrated circuit technologies,<sup>1-5</sup> the fabrication of modified electrodes,<sup>6-15</sup> and the production of various optical components.<sup>16,17</sup> The adhesion problems encountered at metal/dielectric interfaces is clearly illustrated by the difficulty in adhering Au to oxide surfaces. Au is widely accepted as the preferred conductor for integrated circuits, because it has good electrical conductivity properties and is resistant to corrosion, but its applications are limited by its inability to form a strong durable adhesive bond to the dielectric surface. Therefore, typical metal oxide semiconductor field effect transistors (MOSFET) use Al as the metal conductor, because Al and its alloys adhere much better to thermally grown SiO<sub>2</sub> and silicate

glasses.<sup>18</sup> However, there are certain circumstances when Au or an alternate noble metal is required to interface with a dielectric surface, and the means to create a reliable and durable adhesive bond between these metal and oxide surfaces is still needed.

Thin metal films are generally formed by depositing the metal, as a liquid in the form of a sol or by vapor deposition, on the oxide surface and allowing the metal film to solidify. Adhesion between the two surfaces depends on the resultant surface tensions which affect the wetting properties of the solid surface by the liquid. This is shown schematically in Figure 1. The relationship between the forces at the solid/liquid/vapor interface and the wetting properties of the liquid at the solid interface is described by eq 1, where  $s\gamma_v$  is the surface

$$(s\gamma_v - s\gamma_l)/\gamma_v = \cos \theta \quad (1)$$

tension at the solid/vapor interface,  $s\gamma_l$  is the surface tension at the solid/liquid interface,  $\gamma_v$  is the surface tension at the liquid/vapor interface, and  $\theta$  is the contact angle of the liquid at the solid surface. When  $s\gamma_l$  and  $\gamma_v$  are small compared to  $s\gamma_v$ , the contact angle is reduced, and the liquid wets the solid surface. This allows the liquid to adhere to the surface through a variety of different mechanisms such as chemical bond formation and mechanical anchoring. By definition, wetting occurs when the contact angle is  $<90^\circ$  and nonwetting occurs at contact angles  $>90^\circ$ .<sup>19,20</sup>

Au provides an excellent example of the relationship between wetting and adhesion. For instance, the contact angle for Au on an Al<sub>2</sub>O<sub>3</sub> surface is ca. 120° and on silica it is ca. 62°. The surface tension at the Au/Al<sub>2</sub>O<sub>3</sub> interface prevents Au from wetting the Al<sub>2</sub>O<sub>3</sub> surface; as a result, Au does not adhere to the Al<sub>2</sub>O<sub>3</sub> surface.<sup>5</sup> For Au on a SiO<sub>2</sub> surface, the contact angle

\* To whom correspondence should be addressed.

Ⓢ Abstract published in *Advance ACS Abstracts*, December 1, 1994.

(1) Tisone, T. C.; Drobek, J. *J. Vac. Sci. Technol.* **1972**, *9*, 271.

(2) Pretorius, R.; Harris, J. M.; Nicolet, M. A. *Solid-State Electron.* **1978**, *21*, 667.

(3) Ashwell, G. W. B.; Heckingbottom, R. *J. Electrochem. Soc.* **1981**, *128*, 649.

(4) Mitchell, I. V.; Williams, J. S.; Smith, P.; Elliman, R. G. *Appl. Phys. Lett.* **1984**, *44*, 193.

(5) Zdaniewski, W. A.; Silverman, L. D. *J. Mater. Sci.* **1990**, *25*, 3155.

(6) Cohen, R. M.; Janata, J. *J. Electroanal. Chem.* **1983**, *151*, 33.

(7) Sanderson, D. G.; Anderson, L. B. *Anal. Chem.* **1985**, *57*, 2388.

(8) Wehmeyer, K. R.; Deakin, M. R.; Wightman, R. M. *Anal. Chem.* **1985**, *57*, 1913.

(9) Chidsey, G. E.; Feldman, R. J.; Lundren, C.; Murray, R. W. *Anal. Chem.* **1986**, *58*, 601.

(10) Morita, M.; Longmire, M. L.; Murray, R. W. *Anal. Chem.* **1988**, *50*, 2770.

(11) Sabatani, E.; Rubinstein, I.; Maoz, R.; Sagiv, J. *J. Electroanal. Chem.* **1987**, *219*, 365.

(12) Widrig, C. A.; Majda, M. *Anal. Chem.* **1987**, *59*, 754.

(13) Josowicz, M.; Janata, J.; Levy, M. *J. Electrochem. Soc.* **1988**, *135*, 112.

(14) Goss, C. A.; Charych, D. H.; Majda, M. *Anal. Chem.* **1991**, *63*, 85.

(15) Yan, Y.; Bein, T. *J. Phys. Chem.* **1992**, *96*, 9387.

(16) Poate, J. M.; Turner, P. A.; DeBonte, W. J.; Yahalom, J. *J. Appl. Phys.* **1975**, *46*, 4275.

(17) Zydzik, G. J.; Van Uitert, L. G.; Singh, S.; Kyle, T. R. *Appl. Phys. Lett.* **1977**, *31*, 697.

(18) Fraser, D. B. *VLSI Technology*; Sze, S. M., Ed.; McGraw-Hill Book Co.: New York, 1983.

(19) Pask, J. A.; Fulrath, R. M. *J. Am. Ceram. Soc.* **1962**, *45*, 592.

(20) Leedecke, C. J.; Baird, P. C.; Orphanides, K. D. *Electronic Materials Handbook*; Dostal, C. A., Ed.; ASM International: Materials Park, OH, 1993; Vol. 1, p. 453.

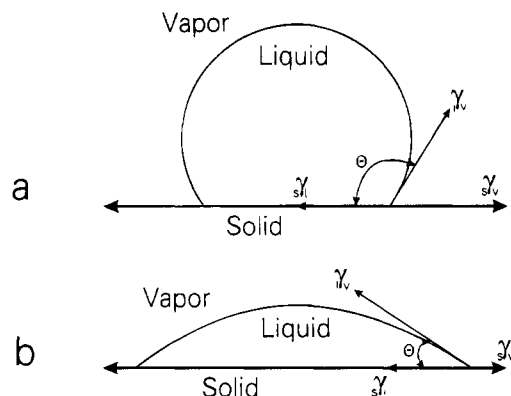


**Figure 1.** Schematic showing wetting angles for (a) nonwetting surface and (b) wetting surface.

suggests that Au only slightly wets the  $\text{SiO}_2$  surface; as a result, Au is poorly adherent to silica.<sup>19</sup>

Adhesion is an attractive force ( $F_{\text{ad}}$ ) exerted between two surfaces and is defined by the energy required to separate the two surfaces a distance  $x$ , as shown in eq 2, where  $W_{\text{ad}}$  is defined by the specific surface energies,

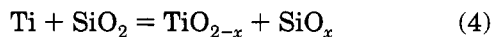
$$W_{\text{ad}} = \int F_{\text{ad}}(x) dx \quad (2)$$

$S_1$  and  $S_2$ , and the interfacial energy,  $S_{1,2}$  of the two materials, as shown in eq 3. From eqs 2 and 3, it can

$$W_{\text{ad}} = S_1 + S_2 - S_{1,2} \quad (3)$$

be seen that  $F_{\text{ad}}$  is greatest when two similar surfaces with high surface energies are in close contact. This situation maximizes the surface energy and minimizes the interfacial energy. Therefore, to improve the adhesion of Au or other noble metals on a dielectric surface, the two surfaces need to be made more compatible in order to minimize the interfacial repulsive forces,  $S_{1,2}$  and  $\gamma_{1,2}$ , which decrease the contact angle.

Several methods have been developed for promoting adhesion between a conducting metal (such as Au, Ag, Pt, and Pd) and a dielectric (such as  $\text{SiO}_2$ ). For example, Ti and other transition metals (such as W, V, Nb, Zr, and Cr) are often used to promote the adhesion of metals to oxides.<sup>2,13</sup> The role of the transition metal is to react with the dielectric material and form a covalently bonded mixed oxide (eq 4), thereby providing a more chemically compatible surface for deposition of a metal film. For Ti on  $\text{SiO}_2$ , this reaction occurs as in eq 4.



Although this approach does improve adhesion, the transition metal has been observed to migrate along grain boundaries within the conducting metal and reach the metal surface, which may be undesirable for certain applications.<sup>1,3,6,17</sup> Pd and Pt have both been used as a barrier layer between the transition metal and the conducting metal to impede the migration process but with only limited success.<sup>1,17</sup>

In other methods, adhesion is promoted by bombarding vapor-deposited metal surfaces with either electrons or ions. Although a complete understanding of how this approach improves adhesion has not been realized, it is generally believed that the impinging ions and electrons provide localized heating at the interface

which facilitates bond formation.<sup>4,21</sup> Oxygen ion-assisted deposition of thin Au films has been shown to improve the adhesion of Au to silica. Adhesion is believed to be enhanced by the formation of a thin metal oxide layer at the metal-dielectric interface, which aids wetting and facilitates bond formation.<sup>22,23</sup>

Several bifunctional organics have also been used to modify oxide surfaces to promote adhesion of vapor-deposited metal films.<sup>24,25</sup> Molecules such as (3-mercaptopropyl)trimethoxysilane,<sup>14,26</sup> 11-trichlorosilylundecyl thioacetate [ $\text{Cl}_3\text{Si}(\text{CH}_2)_{11}\text{SCOCH}_3$ ], and the corresponding thiol<sup>27,28</sup> have two reactive centers, one that will react with an oxide and one that will react with a metal. The bifunctional nature of these organic species improves adhesion by reacting with both surfaces and reducing the repulsive forces at the metal/oxide interface.

The aforementioned studies have been used predominantly to improve the adhesion of thin metal films on thick oxide surfaces. This paper describes a procedure for creating thin oxide films on metal surfaces. The oxide films so created are characterized by ellipsometry, X-ray photoelectron spectroscopy, Raman spectroscopy, and scanning electron microscopy. The adhesion properties are characterized using both qualitative and quantitative adhesion tests. Although the procedures described in this paper are applicable to a variety of dielectric materials for use with either single or multi-component oxide systems including single and multi-layered surfaces, only a silica-based system will be discussed.

## Experimental Section

**Instrumentation.** Raman spectral data were obtained using 100 mW of 514.5 nm radiation from a Coherent Innova 90-5  $\text{Ar}^+$  laser on a Spex 1877 Triplemate spectrometer as described previously.<sup>29-31</sup> The detector in these experiments was a Princeton Instruments charge-coupled device (CCD) system based on a Tektronix TK-512T,  $512 \times 512$ , thinned, back-illuminated, antireflection-coated CCD chip cooled with liquid  $\text{N}_2$  to  $-120^\circ\text{C}$ .

XPS measurements were made using a Vacuum Generators ESCALAB MKII electron spectrometer equipped with a concentric hemispherical analyzer and channeltron electron multiplier. X-rays from an Al  $K\alpha$  source at 1486.6 eV were used for excitation. Electrons were collected in the constant analyzer energy (CAE) mode with a pass energy of 20 keV. Spectra were corrected for sample charging using the C 1s peak at 284.6 eV. Peak areas were calculated using a Gaussian fit program. Relative peak ratios were then calcu-

(21) Werner, B. T.; Vreeland, T.; Mendenhall, M. H.; Qui, Y.; Tombrello, T. A. *Thin Solid Films* **1983**, *104*, 163.

(22) Mattox, D. M. *J. Appl. Phys.* **1966**, *33*, 3613.

(23) Martin, P. J.; Saintry, W. G.; Netterfield, R. P. *Vacuum* **1985**, *35*, 621.

(24) Polniaszek, M. C.; Schauffelberger, R. H. *Adhes. Age* **1968**, *6*, 25.

(25) Allara, D. L.; Nuzzo, R. G. U.S. Patent 4,690,715, 1987.

(26) McGee, J. B. U.S. Patent 4,315,970, 1982.

(27) Wasserman, S. R.; Biebuyck, H.; Whitesides, G. M. *J. Mater. Res.* **1989**, *4*, 886.

(28) Wasserman, S. R.; Tao, Y. T.; Whitesides, G. M. *Langmuir* **1989**, *5*, 1074.

(29) Bryant, M. A.; Pemberton, J. E. *J. Am. Chem. Soc.* **1991**, *113*, 8284.

(30) Pemberton, J. E.; Bryant, M. A.; Sobocinski, R. L.; Joa, S. L. *J. Phys. Chem.* **1992**, *96*, 3776.

(31) Bryant, M. A.; Pemberton, J. E. *J. Am. Chem. Soc.* **1991**, *113*, 3629.

lated using previously published photoionization cross sections.<sup>32</sup>

Ellipsometric measurements were made with a Rudolph Research Model 43603-200E ellipsometer using a He-Ne laser at 632.8 nm at an incident angle of 70°. Readings were taken on bare, vapor-deposited Au and Ag surfaces to establish substrate optical constants prior to surface modification. The Ag surfaces were either used directly after deposition or were sputtered with Ar<sup>+</sup> to remove surface oxides prior to analysis. The surfaces were transferred from the ultrahigh-vacuum chamber and stored for short periods of time in a container purged with UHP argon. A refractive index of 1.45 was used for the 3MPT layer,<sup>33</sup> and a refractive index of 1.46 was used for the thin silica layer.<sup>34</sup> The ellipsometry results were used to calculate the corresponding thickness values using DafiBM version 2.0, a computer program supplied by Rudolph Research and implemented on a DOS-based PC system.

Scanning electron microscopy was performed on a JEOL model 840A system with a tungsten filament at 15.0 kV. The samples were first overcoated with a thin film (5–10 nm) of carbon by vapor deposition prior to analysis.

**Materials.** (3-Mercaptopropyl)trimethoxysilane (3MPT), >95% was purchased from either Hüls America or Aldrich and vacuum distilled prior to use. Tetramethoxysilane (98%) was obtained from Aldrich. Pyridine was UV high-purity grade and purchased from American Burdick and Jackson. Polishing supplies including alumina and polishing pads were purchased from Buehler. HCl was reagent grade and purchased from Baker. Water was obtained from a Milli-Q UV Plus ultrapure Millipore water system. All reagents were used as received unless specified otherwise.

**Methodology.** Adhesion between Ag and Au and an oxide is facilitated with a molecular adhesive, (3-mercaptopropyl)-trimethoxysilane (3MPT). Self-assembled 3MPT films<sup>35</sup> were formed on Ag and Au from a solution of ca. 20 mM thiol/100% ethanol using an immersion time of 2 h. After film formation, the surfaces were rinsed with 100% ethanol and allowed to air dry. Subsequent hydrolysis and condensation of the 3MPT-modified surfaces was accomplished by immersion into an aqueous acid solution (0.1 M HCl) for ca. 12 h. Previous research has shown the presence of a small number of surface silanols associated with the 3MPT monolayer after hydrolysis.<sup>36</sup> We believe that these Si-OH groups provide reaction sites and points of attachment for the thin silica film.

Thin silica films were made by spin casting a dilute, prehydrolyzed tetramethoxysilane (TMOS) solution onto either a 3MPT-modified Ag or Au surface. The TMOS sol was prepared using the recipe of Bertoluzza and co-workers using 4.0 mL of TMOS, 5.5 mL of methanol, 16.3 mL of water, and 0.03 mol of HCl/TMOS.<sup>37</sup> The solution was heated mildly for 0.5 h to facilitate the hydrolysis process. These reaction conditions ensure that all methoxy groups are hydrolyzed and that the viscosity of the solution is suitable for spin casting.

Spin casting of silica films on Ag and Au was accomplished using a Spex sample rotator. After the samples had reached the appropriate spin rate, ca. 3.4 kHz, the prehydrolyzed solution of tetramethoxysilane (TMOS) was applied drop wise (ca. 0.25–0.50 mL/0.30 cm<sup>2</sup>) from a disposable pipet at room temperature. The sample was spun for 1–2 min after deposition. The sample was then removed and placed in a desiccator for 12–24 h.

## Results and Discussion

**Ellipsometry.** Ellipsometry was used to estimate the thickness of the silica films formed using this

**Table 1. Silica Film Thickness Measurements**

	Ag	Au
with 3MPT	87 ± 3 nm	90 ± 8 nm
without 3MPT	0–80 nm	0–2 nm

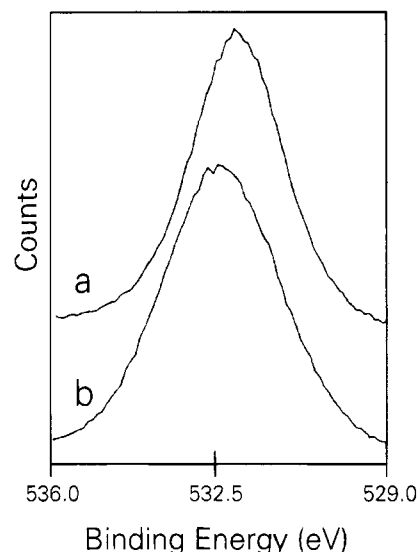


**Figure 2.** Si 2p XPS signal for (a) thin silica layer and (b) chromatographic grade silica.

procedure. Previously reported values for the refractive index of silica sol-gel systems range from 1.28 to 1.46.<sup>38</sup> A refractive index of 1.46 was used for the thickness calculations. This refractive index is consistent with a dense silica gel,<sup>38</sup> such those believed to be formed on the 3MPT-modified Ag and Au surfaces of interest here. Multiple measurements were taken on each sample and at least three samples were used. The data are shown in Table 1. These measurements for the silica films on the 3MPT-modified surfaces indicate film thickness of ca. 87 ± 3 nm on Ag and ca. 90 ± 8 nm on Au. For comparison, if a lower refractive index (such as 1.28) is used in the thickness calculations (which would be consistent with a more porous silica film) the thickness increases by ca. 25 nm.

In the absence of the 3MPT modifier, much different results are obtained. On Au, the silica films that form are patchy at best and give widely varying estimates of silica thickness. On Ag, probably due to the presence of a small amount of native oxide, the silica films are somewhat more reproducible in terms of their observation, but the films are thin and, as will be discussed below, poorly adherent.

**X-ray Photoelectron Spectroscopy.** The chemical nature of the surface of the thin silica films was investigated using X-ray photoelectron spectroscopy (XPS) in order to verify that these films resemble bulk silica. Figure 2 shows the Si 2p signal for the thin silica film (102.4 eV) and a sample of chromatographic grade silica (102.7 eV). The O 1s signal is observed at a binding energy of 532.4 (Figure 3a) for the silica layer and 532.8 eV (Figure 3b) for the chromatographic grade silica. The similarity of the binding energies observed in the XPS spectra between these thin silica films and chromatographic grade silica suggests that the chemical

(32) Scofield, J. H. *J. Electron. Spectrosc. Relat. Phenom.* **1976**, *8*, 129.

(33) Walczak, M. M.; Chung, C.; Stole, S. M.; Widrig, C. A.; Porter, M. D. *J. Am. Chem. Soc.* **1991**, *113*, 2370.

(34) *Handbook of Chemistry and Physics*, 60th ed.; Weast, R. C., Ed.; Chemical Rubber Co.: Boca Raton, FL, 1981.

(35) Thompson, W. R.; Pemberton, J. E. *Langmuir*, submitted.

(36) Thompson, W. R.; Pemberton, J. E. *Chem. Mater.* **1993**, *5*, 241.

(37) Bertoluzza, A.; Fagnano, C.; Morelli, M. A.; Gottardi, V.; Guglielmi, M. *J. Non-Cryst. Solids* **1982**, *48*, 117.

(38) Brinker, C. J.; Scherer, G. W. *Sol-Gel Science: The Physics and Chemistry of Sol-Gel Processing*; Academic Press: New York, 1990; p 767.

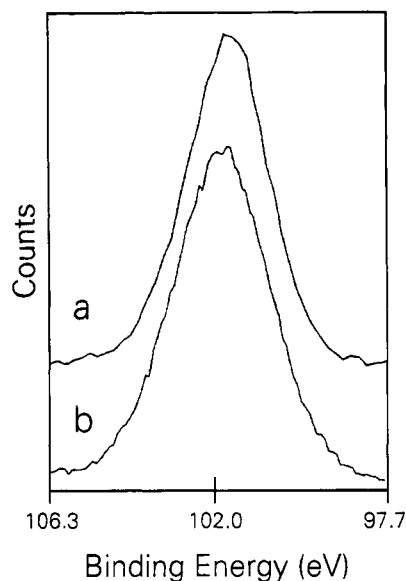


**Figure 3.** O 1s XPS signal for (a) thin silica layer and (b) chromatographic grade silica.

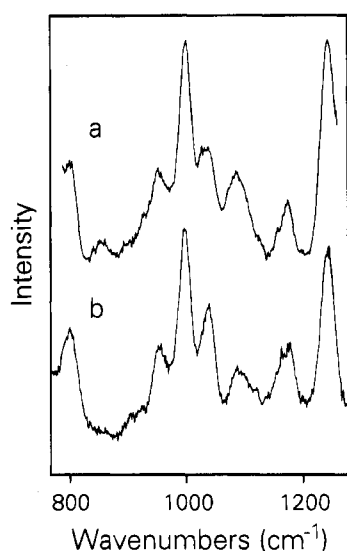


**Figure 4.** Raman spectra in the  $\nu(\text{C}-\text{C})$  region for (a) hydrolyzed, 3MPT-modified Ag surface, (b) thin silica layer on a hydrolyzed, 3MPT-modified Ag surface. Integration times: (a) 90 min and (b) 50 min. Excitation wavelength: (a and b) 514.5 nm.

environment of the thin silica layer is similar to that of bulk silica.<sup>39,40</sup>

**Raman Spectroscopy.** Raman spectra of a monolayer of 3MPT on smooth Ag after hydrolysis and condensation and a thin silica layer on a hydrolyzed, 3MPT-modified Ag surface are shown in Figures 4 and 5, for the  $\nu(\text{C}-\text{C})$  and  $\nu(\text{C}-\text{H})$  regions, respectively. The vibrational assignments of the peaks observed in these spectra are listed in Table 2. The spectrum from the surface of the thin silica film in the  $\nu(\text{C}-\text{C})$  region reveals that the response is dominated by the underlying 3MPT layer, with only minor contributions from the silica. Specifically, the  $\nu(\text{Si}-\text{O}-\text{Si})$  is observed as a weak mode in this spectrum at  $798\text{ cm}^{-1}$ . A similar

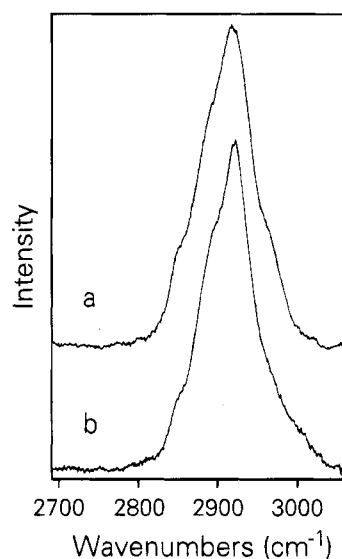


**Figure 5.** Raman spectra in the  $\nu(\text{C}-\text{H})$  region for (a) hydrolyzed, 3MPT-modified Ag surface, (b) thin silica layer on a hydrolyzed, 3MPT-modified Ag surface. Integration times: (a) 10 min and (b) 5 min. Excitation wavelength: (a and b) 514.5 nm.

**Table 2. Raman Frequencies for 3MPT Adsorbed to a Ag Surface after Hydrolysis and Condensation and with Thin Silica Film**

3MPT after H <sup>+</sup> (cm <sup>-1</sup> )	silica film (cm <sup>-1</sup> )	assignment
799	798	$\nu^a(\text{Si}-\text{O}-\text{Si})$
953	953	
998	998	$\nu_s(\text{C}-\text{C})_{\text{T}}^b$
1034	1038	$\nu_s(\text{C}-\text{C})_{\text{T}}$
1083	1083	(CH <sub>2</sub> ) twist <sub>T</sub>
sh	1087	(CH <sub>2</sub> ) twist <sub>T</sub>
c	1117	$\nu(\text{Si}-\text{O}-\text{Si})$
1173	1173	(CH <sub>2</sub> ) twist
1242	1241	(CH <sub>2</sub> ) twist <sub>T</sub>
2854sh <sup>d</sup>	2854sh	$\nu_s(\text{CH}_2)$
2890sh	2891sh	$\nu_s(\text{CH}_2)$
2919	2921	$\nu_s(\text{CH}_2, \text{FR})$
2963sh	sh	$\nu_a(\text{CH}_2)$

<sup>a</sup>  $\nu$  = stretch. <sup>b</sup> T = trans. <sup>c</sup> Not observed. <sup>d</sup> sh = shoulder.

conclusion is drawn from the spectra in the  $\nu(\text{C}-\text{H})$  region. Noteworthy, however, is the fact that in the  $\nu(\text{C}-\text{H})$  region, the  $\nu(\text{C}-\text{H})$  mode associated with the methoxy groups of TMOS at ca.  $2846\text{ cm}^{-1}$  is not present in the spectrum of the thin silica film, further confirming that TMOS is fully hydrolyzed upon silica gel formation.

Raman spectroscopy was also used to evaluate the chemical nature of the surface of the thin silica film using pyridine as a molecular probe. The position of the symmetric ring-breathing vibration of pyridine,  $\nu_1$ , is extremely sensitive to the chemical environment of the lone-pair electrons of the nitrogen.<sup>41-43</sup> The more strongly interacting the lone pair of electrons, the larger the shift in  $\nu_1$  to higher frequencies, as shown in Table 3.

As shown by the spectra in Figure 6, the symmetric ring-breathing vibration of pyridine,  $\nu_1$ , shifts from ca.  $991\text{ cm}^{-1}$  in neat pyridine to ca.  $1011\text{ cm}^{-1}$  upon

(39) Carley, F. A.; Moroney, L.; Roberts, M. W. *Faraday Discuss. Chem. Soc.* **1980**, *15*, 39.

(40) Nasu, H.; Heo, J.; Mackenzie, J. D. *J. Non-Cryst. Solids* **1988**, *99*, 140.

(41) Wilhurst, R. K.; Bernstein, H. J. *Can. J. Chem.* **1957**, *35*, 1183.

(42) Eagerton, T. A.; Hardin, A. H.; Kozirovski, Y.; Sheppard, N. J. *J. Catal.* **1974**, *32*, 343.

(43) Hendra, P. J.; Horder, J. R.; Loader, E. J. *J. Chem. Soc. A* **1971**, 1766.

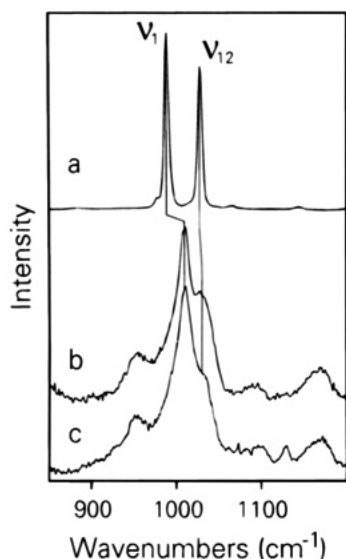


**Figure 6.** Raman spectra in the "ring breathing" region of (a) neat pyridine, (b) pyridine adsorbed to the thin silica film from  $\text{CCl}_4$ , and (c) pyridine adsorbed to the thin silica film from  $\text{H}_2\text{O}$ . Integration times: (a) 0.25 min, (b) 10 min, and (c) 10 min. Excitation wavelength: (a-c) 514.5 nm.

**Table 3. Pyridine Vibrational Behavior**

pyridine environment	$\nu_1$ ( $\text{cm}^{-1}$ )	$\nu_{12}$ ( $\text{cm}^{-1}$ )	mode of interaction	ref
pyridine (neat)	991	1030		41-43
pyridine/ $\text{CCl}_4$	991	1031	no interaction	42, 43
pyridine/ $\text{H}_2\text{O}$	1003	1036	H-bonding	42, 43
pyridine/chromatographic grade silica (low coverage)	1010	1035	H-bonding	42, 43
pyridine/chromatographic grade silica (high coverage)	991	1031	physisorption	42
obsd: neat pyridine	991	1028		
obsd: pyridine adsorbed from $\text{CCl}_4$	1011	1030	H-bonding	
obsd: pyridine adsorbed from $\text{H}_2\text{O}$	1011	1031	H-bonding	

adsorption to the thin silica film. The shift in frequency for  $\nu_1$  in Figures 6a,b suggests that pyridine is adsorbed at surface silanols, which are Brønsted acid sites, through the nitrogen atom from both aqueous and  $\text{CCl}_4$  solutions. The additional bands in Figure 6 are 3MPT and silica vibrations, as mentioned previously.

The trigonal ring-breathing mode,  $\nu_{12}$ , at ca. 1032  $\text{cm}^{-1}$  in neat pyridine, is less sensitive to chemical environment but does shift ca. 3  $\text{cm}^{-1}$  toward higher frequencies. However, the lower relative intensity of the  $\nu_{12}$  band for pyridine adsorbed from aqueous solution (Figure 6c) is consistent with additional hydrogen bonding as compared to the spectrum observed from pyridine adsorbed from a  $\text{CCl}_4$  solution.<sup>44</sup> Peaks associated with bulk pyridine are not present in either spectrum, suggesting that only a monolayer of pyridine is present on the silica surface. The Raman spectral results for pyridine on these thin silica films are similar to those observed on other silica surfaces.

**Scanning Electron Microscopy.** The surfaces of the thin silica films were further characterized by scanning electron microscopy (SEM). Figures 7-10 show the SEM images of a bare, polished Ag surface, a

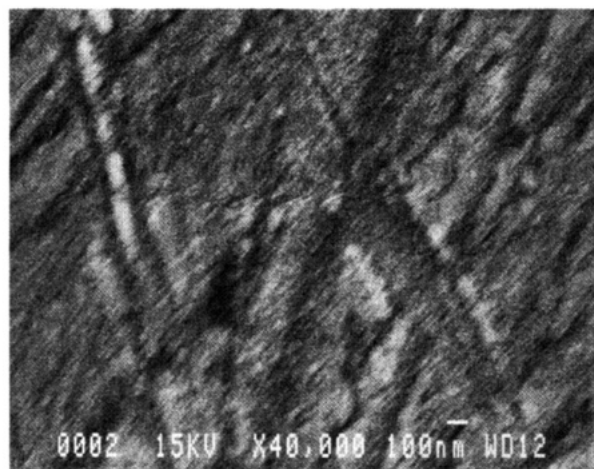
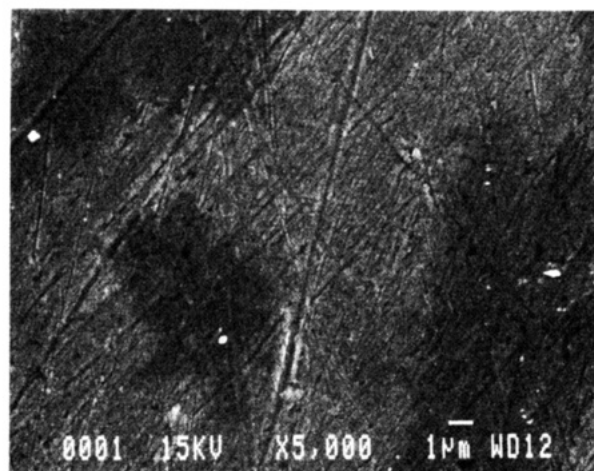


**Figure 7.** SEM image of bare a Ag surface at (a) low magnification and (b) high magnification.

3MPT-modified Ag surface, a hydrolyzed, 3MPT-modified Ag surface, and a thin silica layer on a hydrolyzed, 3MPT-modified Ag surface, respectively.

The darker areas which are observed on the SEM image of the bare Ag surface (Figure 7) are believed to be due to the presence of a small amount of surface oxide. SEM analysis could not be performed immediately after polishing, and therefore, the surfaces were exposed to the ambient environment for several hours. The corrugated lines on this surface are roughness features formed by mechanical polishing of the metal surface and appear in all the SEM images. The 3MPT-modified Ag surface did not appear to be oxidized and dark patches, similar to those in Figure 7, were not observed in the SEM image of the 3MPT-modified Ag surface (Figure 8). The SEM image of the hydrolyzed, 3MPT-modified Ag surface (Figure 9) appears similar to the previous two surfaces, except for several small surface features, which are more clearly observed in the high-resolution SEM image (Figure 9b). The small particles are formed after the surfaces are immersed in aqueous acid solution and may be residual salts. Upon spin casting of the thin silica film on the modified Ag surface (Figure 10), the SEM image indicates that the thin silica film conforms to the roughness of the underlying Ag surface and appears to be uniform, fairly dense, and thin.

**Adhesion.** Methods typically used for the measurement of adhesion are designed to cause a mechanical stress at the interface and typically depend on applica-

(44) Kagel, R. O. *J. Phys. Chem.* **1970**, *74*, 4518.

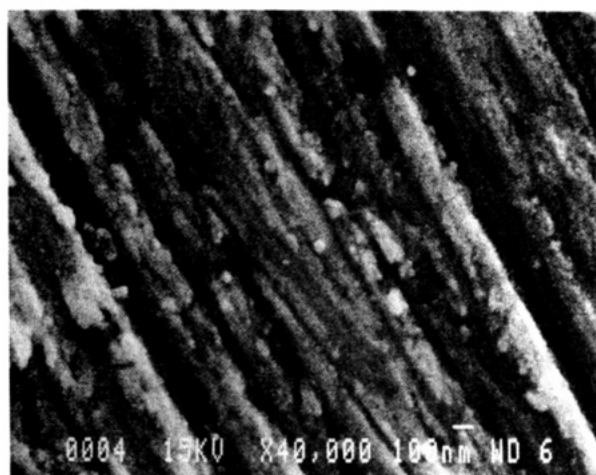
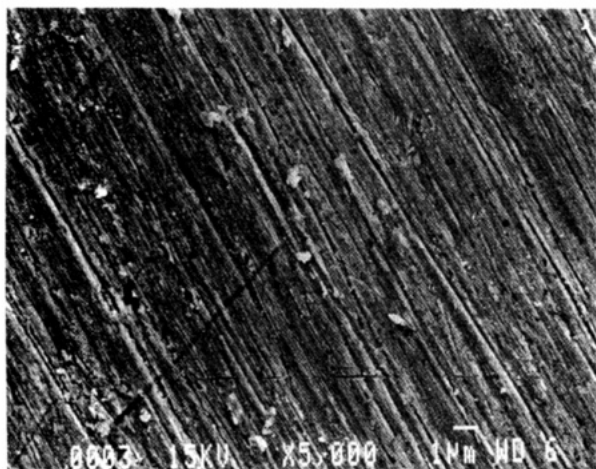


**Figure 8.** SEM image of 3MPT-modified Ag surface at (a) low magnification and (b) high magnification.

tion of a measurable or known force to the overlayer. If the mechanical stresses exceed the adhesive forces between the two materials, an adhesive failure at the interface is observed. The mechanical stresses applied to the overlayer can either be tensile (perpendicular to the interface) or shear (parallel to the interface). Several tests have been developed to measure adhesion such as the Scotch tape test (qualitative), abrasion test (qualitative), the stud pull test (quantitative), and the scratch test (quantitative).<sup>45</sup>

Several types of adhesion tests were performed on our thin silica films in an attempt to quantify their adhesion to both the 3MPT-modified and unmodified metal surfaces. Stud pull tests were performed by Adhesion International, Division of Quad Group, Inc. Qualitative tests were performed in this laboratory and interpreted according to the methods of Mattox.<sup>22</sup>

Mattox has previously correlated common qualitative tests with a Kentron microhardness tester modified to measure scratch resistance, while investigating the adhesion of thin Au films on a silica surface in the presence of an O<sub>2</sub> environment.<sup>22</sup> He concluded that films which fail the tape test also fail the scratch test with a load of 5 g or less and have been defined as poorly adhering. Moderately adherent films fail the scratch test with a load of between 25 and 100 g. These films pass the tape test but can be removed by abrading the

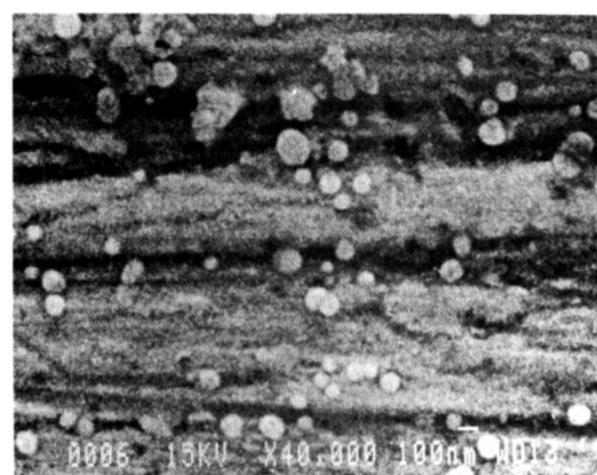
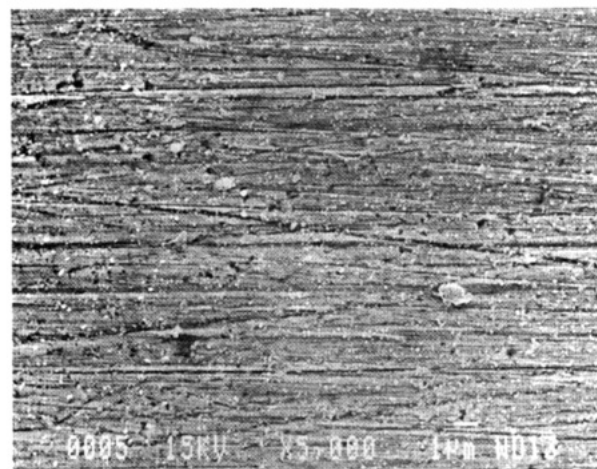


**Figure 9.** SEM image of hydrolyzed 3MPT-modified Ag surface at (a) low magnification and (b) high magnification.

film with the point of a pencil. Highly adherent films resist scratch damage with a load in excess of 600 g and can be scratched with a sharp point without removing all of the overlayer.

Thin silica films formed from TMOS solution on bare (unmodified) Au surfaces were found to be poorly adherent on the basis of visual observations and ellipsometric measurements. When using unmodified Au surfaces, the majority of the TMOS solution was spun off during the spin coating procedure leaving small islands of silica on the Au surface. Ellipsometric measurements of the unmodified Au after spin coating with the TMOS solution indicate that the silica film thicknesses were between ca. 0 and 20 Å, not including the small silica islands which were too small to measure. These silica islands were able to withstand tape tests but did not remain attached after tapping the surface with the point of a pencil. The tape tests were performed by firmly placing a piece of Scotch tape (Magic Tape 810) across the entire sample and manually removing the tape at 90° with respect surface normal at ca. 1 cm/s. On the basis of these collective results, the silica islands films can be classified as poorly adhering, although the silica islands themselves can be classified as moderately adhering.

On unmodified Ag surfaces, the TMOS solution wets the Ag surface effectively creating an adherent silica layer. However, the silica films formed on the unmodified Ag surfaces were uneven and had thicknesses

(45) Pulker, H. K. *Coatings on Glass*; Elsevier: New York, 1984.

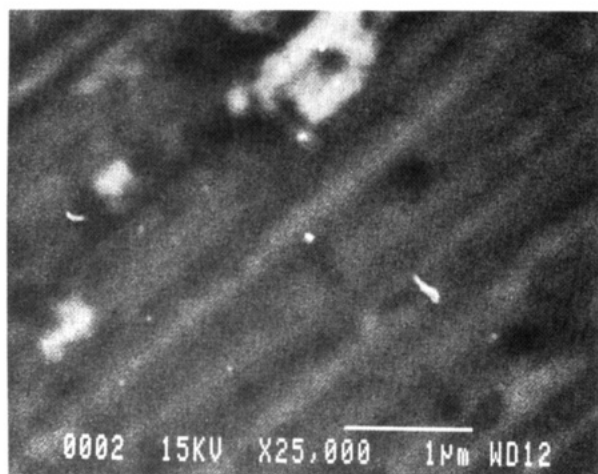
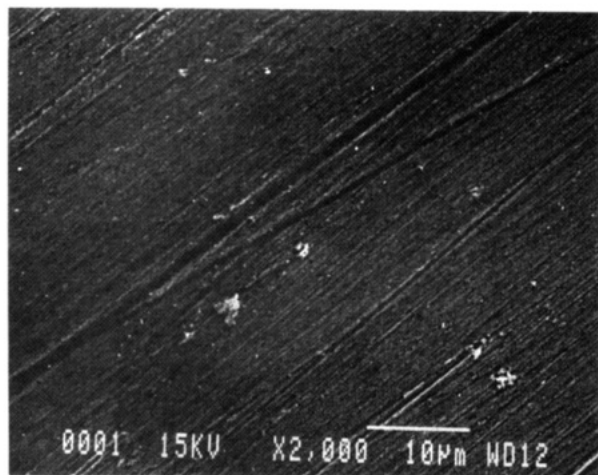


**Figure 10.** SEM image of thin silica film on hydrolyzed 3MPT-modified Ag surface at (a) low magnification and (b) high magnification.

between ca. 0 and 80 nm. These silica films were able to withstand the tape test but were scratched off with a point of a pencil. According to the observations of Mattox, these thin silica films are moderately adhering. The native oxide layer on the Ag surface is believed to act as an adhesive for the attachment of the silica film. Au does not readily form an oxide layer; therefore, the silica does not adhere to the Au surface as well.

Silica films formed on 3MPT-modified Ag and Au surfaces were able to withstand tape tests and abrading with the point of a pencil. A sharper object such as a razor blade penetrated the silica surface and scratched the underlying Ag and Au surfaces. However, this

abrasion did not cause the surrounding silica overlayer to flake off. Therefore, the silica films formed on 3MPT-modified Ag and Au surfaces are classified as highly adhering according to the scheme proposed by Mattox. Adhesion was maintained even after heating the samples to 150 °C in a vacuum oven at 635 mmHg.

Stud pull tests were performed in order to provide a more quantitative assessment of the adhesion between the thin silica layer and the 3MPT-modified Ag surface. In this test, metal studs are attached to the surface of interest using a thin epoxy film. The stud is then pulled perpendicular to the surface until the stud detaches. A maximum load of 11.33 kpsi was achieved before separation. Epoxy was left on both the silica surface and the stud surface, suggesting that adhesion failed due to a cohesive failure within the epoxy and not due to rupture of the 3MPT molecular layer or the thin silica film.

It is believed that the strong adhesive nature of these systems is due in part to the densely packed, highly ordered nature of the 3MPT monolayer on the metal surface, as well as the ability of 3MPT to covalently bond to both the metal surface and the oxide. In addition, residual hydroxyls on the hydrolyzed 3MPT surface allow the TMOS solution to more completely wet the metal surface, and provide for more even film formation.<sup>46</sup>

### Conclusions

The results presented here demonstrate that organosilanes can be used to modify metal surfaces in order to attach thin silica layers to Ag and Au surfaces. This approach can easily be applied to a variety of different single and multilayered sol-gel systems, as well as metal surfaces. The thin silica surfaces formed by this method have been shown to be representative of other silica systems. The adhesion between these two surfaces is accomplished through the chemical attachment of the silica layer to the metal surface by a molecular adhesive. If the molecular adhesive was not used, the silica layer did not adhere as effectively to the metal surface.

**Acknowledgment.** The authors gratefully acknowledge support of this work by the National Science Foundation (CHE-9121469 and CHE-9023678).

CM940335D

(46) Thompson, W. R.; Pemberton, J. E. *Anal. Chem.* **1994**, *66*, 3362.